Theory of X-ray scattering in the anomalous dispersion region and the problem of atomic-ternary-correlation-function determination in amorphous media

1992 J. Phys.: Condens. Matter 4 6155

(http://iopscience.iop.org/0953-8984/4/28/016)

J. Phys.: Condens. Matter 4 (1992) 6155–6169. Printed in the UK

Theory of x-ray scattering in the anomalous dispersion region and the problem of atomic-ternary-correlation-function determination in amorphous media

R V Vedrinskii, V L Kraizman, A A Novakovich and V Sh Machavariani

Theoretical Department of the Institute of Physics, Rostov State University, Stachky Ave. 194, 344 104, Rostov-on-Don, Russia

Received 22 October 1991

Abstract. A new method for x-ray atomic scattering factor (ASF) calculations in solids is proposed which enables one to obtain imaginary and real parts of the ASF without Kramers–Krönig transformation in the anomalous dispersion region (both in XANES and EXAFS regions). The method proposed allows for the inclusion of the environmental influence upon the ASF of the atoms in solids. Due to such influence, ASF in general becomes an anisotropic tensor. As an example, the ASF tensor components of a boron atom in a hexagonal BN crystal are calculated near the B K absorption edge. Imaginary parts of the ASF tensor components are employed to calculate the XANES which appears to be in reasonable agreement with experiment. The formulae for the intensity of x-ray diffraction from a homoatomic thin amorphous sample in a K-edge EXAFS region are obtained. The environmental influence upon the ASF causes the fine structure in the frequency dependence of the x-ray diffraction intensity. This fine structure together with the angular dependence of diffraction intensity is shown to provide valuable information about atomic ternary correlation functions of amorphous media.

1. Introduction

X-ray scattering in condensed matter in a normal dispersion region of photon energy can be described satisfactorily within the framework of the free atom approach to the calculation of the atomic scattering factors (ASFs) [1]. In this frequency region only the small corrections caused by the difference between real crystalline electronic density and superposition of atomic densities of free atoms should be involved. However, if the photon energy is near the absorption edge of any atomic core level, the ASF depends appreciably on the chemical state and environment of the scattering atoms, as does the x-ray absorption cross-section in the near edge region, this being shown to be caused by scattering of the photoelectrons from the neighbouring atoms. In the case of the x-ray elastic scattering process real (photo) electrons do not appear in the final state, but in the intermediate state the virtual electrons exist. Due to the virtual electron interaction with surrounding atoms the ASF becomes an anisotropic tensor with sharp photon energy dependence in the anomalous dispersion region. Anisotropy of the ASF leads to a number of well known phenomena such as pleochroism, existence of 'structurally forbidden' reflections [2, 3], birefringence, orientational dependence of XANES [4], reflectivity [5]

0953-8984/92/286155 + 15 $04.50

etc. The analysis of such experimental phenomena allows one to obtain important information about the atomic structure of the substances investigated. The energy dependence of the ASF in solids was treated in papers [6–8] by Kramers–Krönig transformation of EXAFS, and the explicit formula for ASF fine structure was obtained, but the method proposed in these papers cannot be used in near edge regions. Besides, only the case of unpolarized radiation was considered in [6–8], hence anisotropy of the ASF was not treated.

In section 2 a new method based on Green's function formalism is proposed for ASF calculations. A simple expression for the ASF derived there allows *ab initio* computation of the ASF in the near edge region without using Kramers–Krönig transformation. An explicit EXAFS-like formula for extended fine structure of the ASF is also presented. In section 3, the ASF tensor of a boron atom in a hexagonal BN crystal is calculated near the B K edge as an example of the method proposed. The imaginary part of this factor appears to be in reasonable agreement with experimental XANES. In section 4 the expressions for energy and angular dependence of x-ray scattering intensity are derived for the case of amorphous samples in the EXAFS region. Such dependence is shown to be the source of valuable information about atomic ternary correlation functions in amorphous media.

2. The atomic scattering factor in the anomalous dispersion region

For the sake of simplicity we suppose the photon energy to be close to the K absorption edge of the scattering atom. In this case, the atomic polarizability tensor $\chi_{\alpha\beta}$ can be divided into two parts: an anomalous part $\chi^{\mathrm{an}}_{\alpha\beta}$ which is due to 1s shell polarization, and a normal part $\chi^{\mathrm{norm}}_{\alpha\beta}$ which is caused by the polarization of all other electrons:

$$\chi_{\alpha\beta} = \chi^{\mathrm{norm}}_{\alpha\beta} + \chi^{\mathrm{an}}_{\alpha\beta}. \tag{1}$$

Hereafter the tensor components will be denoted by Greek subscripts.

If the photon energy is close to the K edge it exceeds the ionization energies of all other shells by a considerable amount. Therefore, the tensor $\chi^{\mathrm{norm}}_{\alpha\beta}$ can be obtained within the traditional semiclassical approximation [1]. However, the polarizability of the 1s shell in the dipole approximation is described by the well known quantum formula [1]:

$$\chi^{\mathrm{an}}_{\alpha\beta} = -2e^2 \sum_{\substack{n \\ E_n > E_{\mathrm{F}}}} \frac{\langle 1\mathrm{s}|\hat{r}_\alpha|n\rangle\langle n|\hat{r}_\beta|1\mathrm{s}\rangle}{\hbar\omega + E_{1\mathrm{s}} - E_n + \mathrm{i}\Gamma/2} + 2e^2 \sum_{\substack{n \\ E_n > E_{\mathrm{F}}}} \frac{\langle 1\mathrm{s}|\hat{r}_\beta|n\rangle\langle n|\hat{r}_\alpha|1\mathrm{s}\rangle}{\hbar\omega - E_{1\mathrm{s}} + E_n + \mathrm{i}\Gamma/2} \tag{2}$$

where $\hbar\omega$ is the photon energy, e is the electron charge, $|n\rangle$ and E_n are an eigenfunction and an eigenvalue of the one-electron Hamiltonian, E_{F} is the Fermi-level energy, $\hat{r}_\alpha$ is the position operator, Γ is the width of the excited state with a hole in the 1s shell and an electron in the $|n\rangle$ state (we assume for simplicity that Γ does not depend on n).

If the photon energy is close to the K absorption edge, the second term in (2) is small and the anomalous part of the ASF can be written as follows:

$$f^{\mathrm{an}}_{\alpha\beta} = -\frac{\omega^2}{c^2 r_0}\chi^{\mathrm{an}}_{\alpha\beta} = 2m\omega^2 \sum_{\substack{n \\ E_n > E_{\mathrm{F}}}} \frac{\langle 1\mathrm{s}|\hat{r}_\alpha|n\rangle\langle n|\hat{r}_\beta|1\mathrm{s}\rangle}{\hbar\omega + E_{1\mathrm{s}} - E_n + \mathrm{i}\Gamma/2} \tag{3}$$

where r_0 is the electron classical radius, m is the electron mass and c is the velocity of light.

Straightforward calculation of the ASF based on expression (3) is difficult because of the infinite degeneracy of the eigenvalues E_n and the complicated character of the electron wave functions calculated in polyatomic system potentials. Similar difficulties appear in the theory of x-ray absorption fine structure where the one-electron Green's function (GF) method is shown to be very convenient [9, 10]. It will be shown below that this method also permits simplification of the formula (3) and development of the new approach to ASF theory to allow the calculation of the tensor $f^{an}_{\alpha\beta}$ without using Kramers–Krönig transformation.

The one-electron GF is defined in the usual way [11]

$$G(\varepsilon) = \sum_n \frac{|n\rangle\langle n|}{\varepsilon - E_n}. \tag{4}$$

In order to calculate expression (3) using the definition (4) of GF one should carry out the summation in the right-hand part of (3) over all n and then subtract the sum over filled electron states:

$$\begin{aligned} f^{an}_{\alpha\beta} &= 2m\omega^2\langle 1s|\hat{r}_\alpha\left(\sum_n \frac{|n\rangle\langle n|}{\hbar\omega + E_{1s} - E_n + i\Gamma/2}\right)\hat{r}_\beta|1s\rangle \\ &\quad - 2m\omega^2 \sum_{\substack{n \\ E_n < E_F}} \frac{\langle 1s|\hat{r}_\alpha|n\rangle\langle n|\hat{r}_\beta|1s\rangle}{\hbar\omega + E_{1s} - E_n + i\Gamma/2} \\ &= 2m\omega^2\langle 1s|\hat{r}_\alpha G(\hbar\omega + E_{1s} + i\Gamma/2)\hat{r}_\beta|1s\rangle \\ &\quad - 2m\omega^2 \int_{-\infty}^{E_F} \langle 1s|\hat{r}_\alpha\left(\sum_n \frac{|n\rangle\langle n|\,\delta(\varepsilon - E_n)}{\hbar\omega + E_{1s} - \varepsilon + i\Gamma/2}\right)\hat{r}_\beta|1s\rangle\,d\varepsilon \\ &= 2m\omega^2\langle 1s|\hat{r}_\alpha G(\hbar\omega + E_{1s} + i\Gamma/2)\hat{r}_\beta|1s\rangle \\ &\quad + \frac{m\omega^2}{i\pi}\int_{-\infty}^{E_F} \frac{\langle 1s|\hat{r}_\alpha[G(\varepsilon - i\eta) - G(\varepsilon + i\eta)]\hat{r}_\beta|1s\rangle}{\hbar\omega + E_{1s} - \varepsilon + i\Gamma/2}\,d\varepsilon. \end{aligned} \tag{5}$$

Here we have used the well known relation for the GF discontinuity at a real axis [11]

$$G(\varepsilon + i\eta) - G(\varepsilon - i\eta) = -2\pi i \sum_n |n\rangle\langle n|\,\delta(\varepsilon - E_n)$$

where η is a positive infinitesimal constant.

The second term in the right-hand part of (5) can be written as follows:

$$\frac{m\omega^2}{i\pi}\int_{\mathcal{L}} \frac{\langle 1s|\hat{r}_\alpha G(\varepsilon)\hat{r}_\beta|1s\rangle}{\hbar\omega + E_{1s} - \varepsilon + i\Gamma/2}\,d\varepsilon \tag{6}$$

where $\mathcal{L}$ is the path in the complex energy plane shown in figure 1.

At a real axis of the complex energy plane, the GF $G(\varepsilon)$ has poles when ε is equal to the bound state energies and may also have sharp maxima in the valence band region, hence straightforward numerical calculations of expression (6) are complicated. It is convenient to rewrite expressions (5) and (6) so that one can use the path $\mathcal{L}_1$ shown in figure 1 instead of $\mathcal{L}$ where the path $\mathcal{L}_1$ envelopes the energies of all filled electron states and Γ_1 is greater than Γ. The GF, $G(\varepsilon)$, is a smooth function of ε along the path $\mathcal{L}_1$ that significantly simplifies the numerical calculations of the integral term in (5).

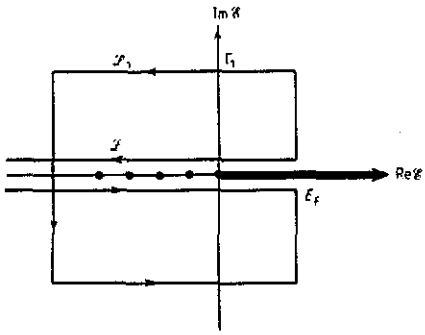

Figure 1. The paths $\mathscr{L}$ and $\mathscr{L}_1$ in the complex energy plane used in formulae (6) and (7). The beginning and the final points of both paths are $E_F \pm i0$. Discrete and continuous parts of the one-electron Hamiltonian spectrum are shown on the real axis.

Finally, the anomalous part of the ASF can be expressed in the form

$$f_{\alpha\beta}^{an} = 2m\omega^2\langle 1s|\hat{r}_\alpha\, G(\hbar\omega + E_{1s} + i\Gamma/2)\,\hat{r}_\beta|1s\rangle\,\theta(\hbar\omega + E_{1s} - E_F) + \frac{m\omega^2}{i\pi}\int_{\mathscr{L}_1}\frac{\langle 1s|\hat{r}_\alpha\, G(\varepsilon)\,\hat{r}_\beta|1s\rangle}{\hbar\omega + E_{1s} - \varepsilon + i\Gamma/2}\,d\varepsilon \tag{7}$$

where

$$\theta(x) = \begin{cases} 1 & \text{if } x > 0 \\ 0 & \text{if } x < 0. \end{cases}$$

It is worth noting that the ASF is an unbroken function of the electron energy $(\hbar\omega + E_{1s})$ at the Fermi level, though both terms in the right-hand part of (7) have discontinuities at this point.

The GF of the electron in a polyatomic system could be calculated easily if the muffin-tin approximation for the one-electron potential was used [9, 10]. Due to strong localization of the 1s wave function one has to know the GF $G(\boldsymbol{r}, \boldsymbol{r}', \varepsilon)$ in (7) only for the arguments $\boldsymbol{r}$ and $\boldsymbol{r}'$ lying within the scattering atom sphere. In this case, the following expansion for the GF takes place [10]:

$$G(\boldsymbol{r}, \boldsymbol{r}', \varepsilon) = G^0(\boldsymbol{r}, \boldsymbol{r}', \varepsilon) + \frac{2mk}{\hbar^2}\sum_{L,L'}\exp[(i(\delta_l^n + \delta_{l'}^n)]G_{LL'}^{nn}(\varepsilon) \times R_l^n(\varepsilon, r)Y_L(\Omega_r)R_{l'}^n(\varepsilon, r')Y_{L'}(\Omega_{r'}) \tag{8}$$

where $G^0(\boldsymbol{r}, \boldsymbol{r}', \varepsilon)$ is the electron GF calculated for the isolated atomic sphere of the scattering atom, $R_l^n(r)$ is the regular solution of the radial Schroedinger equation for atom number n, δ_l^n is the partial scattering phase shift, l is the electron angular momentum, n is the scattering atom number, $L \equiv (l, m)$ and $Y_L(\Omega_r)$ is the real spherical harmonic. Hereafter, the origin of the electron energy ε is combined with the muffin-tin zero: $k = (2m\varepsilon/\hbar^2)^{1/2}$. The coefficients $G_{LL''}^{nn''}$ could be determined from the system of algebraic equations [9, 10]:

$$G_{LL''}^{nn''} = g_{LL''}^{nn''} + \sum_{L'}\sum_{n'} g_{LL'}^{nn'}t_{l'}^{n'}G_{L'L''}^{n'n''} \tag{9}$$

where $t_l^n = -\sin(\delta_l^n)\exp(i\delta_l^n)$

and

$$g_{LL'}^{nn'} = 4\pi \sum_{L''} i^{l''+l'-l-1} h_{l''}^{(1)}(kr_{nn'}) Y_{L''}\,[\Omega_{r_{nn'}}] \int Y_L(\Omega_r) Y_{L'}(\Omega_r) Y_{L''}(\Omega_r)\,\mathrm{d}\Omega.$$

If one substitutes the expansion (8) for the expression (7), the anomalous correction $f_{\alpha\beta}^{\mathrm{an}}$ to the ASF can be divided into two parts:

$$f_{\alpha\beta}^{\mathrm{an}} = \Delta f^{(0)} \delta_{\alpha\beta} + \Delta f_{\alpha\beta}^{(1)} \tag{10}$$

where

$$\Delta f^{(0)} = \tfrac{2}{3} m\omega^2 < 1\mathrm{s}|r\,G^0(\hbar\omega + E_{1\mathrm{s}} + \mathrm{i}\Gamma/2)\,r|1\mathrm{s} > \theta(\hbar\omega + E_{1\mathrm{s}} - E_{\mathrm{F}})$$
$$+ \frac{m\omega^2}{3\pi\mathrm{i}} \int_{\mathscr{L}_1} \frac{\langle 1\mathrm{s}|r\,G^0(\varepsilon)r|1\mathrm{s}\rangle}{\hbar\omega + E_{1\mathrm{s}} - \varepsilon + \mathrm{i}\Gamma/2}\,\mathrm{d}\varepsilon \tag{11}$$

is an isolated atomic-sphere anomalous correction.

The sum

$$f^{\mathrm{norm}} + \Delta f^{(0)} = f^{\mathrm{isol}} \tag{12}$$

is the total scattering factor of the isolated atomic sphere. The difference between the isolated atomic sphere scattering factor and that of the free atom will be considered in the following section.

The second part of the anomalous correction $\Delta f_{\alpha\beta}^{(1)}$ appears to be due to virtual electron scattering from the atoms surrounding the scattering one. Therefore, it could be called the virtual electron scattering correction (VESC). This correction is in general the anisotropic tensor, in contrast to the atomic-sphere contribution $\Delta f^{(0)}\delta_{\alpha\beta}$. Taking into account dipole selection rules, one can write the following expression for the VESC of the atom located at point r_n

$$\Delta f_{\alpha\beta}^{(1)}(\omega, r_n) = (2m\omega/\hbar)^2\,(k/3) \left\{ G_{\alpha\beta}^{nn}(\varepsilon_f) M_{01}^2(\varepsilon_f)\,\mathrm{e}^{2\mathrm{i}\delta_1^n(\varepsilon_f)}\,\theta(\hbar\omega + E_{1\mathrm{s}} - E_{\mathrm{F}}) \right.$$
$$\left. + \frac{1}{2\pi\mathrm{i}} \int_{\mathscr{L}_1} \frac{M_{01}^2(\varepsilon) G_{\alpha\beta}(\varepsilon)\,\mathrm{e}^{2\mathrm{i}\delta_1^n(\varepsilon)}}{\varepsilon_f - \varepsilon}\,\mathrm{d}\varepsilon \right\} \tag{13}$$

where $\varepsilon_f = \hbar\omega + E_{1s} + \mathrm{i}\Gamma/2$. $M_{01}(\varepsilon) = \int \varphi_{1s}(r) r^3 R_1(\varepsilon, r)\,\mathrm{d}r$. Vector subscripts α, β instead of L, L' appear in (13) because real spherical harmonics $Y_{lm}(\Omega_r)$ for $l = 1$ coincide with the components of the vector r/r; hence, in this case, one can denote the angular harmonics by $Y_\alpha(\Omega_r)$ and the corresponding coefficients $G_{LL'}^{nn}$ by $G_{\alpha\beta}^{nn}$.

Above the 1s threshold, the integral term in (13) is a smooth function of photon energy that decreases as $(\hbar\omega + E_{1\mathrm{s}} - E_{\mathrm{F}})^{-1}$, hence the ASF fine structure appears due to only the first term in the braces in (13). Keeping in mind the similarity between this term and XANES one can say that the ASF fine structure in the near edge region is caused by multiple scattering of virtual electrons from the neighbouring atoms.

If the photon energy exceeds the absorption edge by more than 20–50 eV, the single-scattering approximation is usually valid to describe the interaction of both real photo and virtual electrons with neighbouring atoms [12]. (Exceptions to this rule were treated in EXAFS theory [12–14].) In this energy region, partial scattering amplitudes t_l^n are small

and the first iteration of equation (9) gives a good approximation for the electron GF [15, 16]

$$G^{nn}_{LL'}(\varepsilon_f) \approx -\frac{4\pi}{k} i^{-l} i^{l'} \sum_{\substack{q \\ q \neq n}} Y_L(\Omega_{r_{nq}}) Y_{L'}(\Omega_{r_{qn}}) \exp(2ikr_{nq}) \exp(-m\Gamma r_{nq}/\hbar^2 k) F^q(\pi)/r^2_{nq} \tag{14}$$

where $F^q(\pi) = -(1/k)\,\Sigma_l(2l+1)P_l(-1)t_l^q$ is the electron backscattering amplitude, $r_{nq} = r_q - r_n$, r_n is the radius vector of the nth atom, $k = [2m(\hbar\omega + E_{1s} - E_0)]^{1/2}/\hbar$ is the electron wave vector, E_0 is the muffin-tin zero and $P_l(\cos\theta)$ is the Legendre polynomial.

Using the single-scattering approximation (14) for the GF and neglecting the rapidly decreasing integral term in (13), one obtains an explicit expression for the VESC in the extended fine structure region:

$$\Delta f^{(1)}_{\alpha\beta}(\omega, r_n) = \left(\frac{2m\omega M_{01}}{\hbar}\right)^2 \sum_{\substack{q \\ q \neq n}} (r_{nq})_\alpha (r_{nq})_\beta \exp\left(2ikr_{nq} + 2i\delta_1^n - \frac{m\Gamma r_{nq}}{\hbar^2 k}\right) F^q(\pi)/r^4_{nq}. \tag{15}$$

In cubic crystals, the ASF is the isotropic tensor, and in this case the expression (15) is similar to that obtained earlier [6–8] by Kramers–Krönig transformation. Contrary to this case, the expression (15) is valid for crystals of any symmetry and amorphous media as well. In section 4 we show, by exploiting (15), that the intensity of the radiation scattered from the amorphous samples is determined by pair and ternary atomic distribution functions that give the opportunity to obtain information about these functions from the experimental spectra.

3. Calculation of the ASF tensor for a boron atom in a hexagonal BN crystal

In order to illustrate the theory developed here we have calculated the boron atom scattering factor in a hexagonal BN (h-BN) crystal near a B K absorption edge. It was shown in [17] that the near edge fine structure of B K absorption spectra in h-BN has a number of prominent features. In the case of monocrystal samples the intensities of these features depend appreciably on the direction of the electric field vector if linearly polarized radiation is employed [18, 19]. Keeping in mind these characteristic features of XANES one can expect that the ASF of a boron atom in h-BN is the anisotropic tensor and that its components depend sharply on the photon energy near the B K absorption edge.

The crystal structure of h-BN is graphite-like [20], therefore this crystal is dichroic. If one directs the z-axis of the coordinate system along the principal optical axis of the crystal, the ASF tensor will be diagonal and $f_{xx} = f_{yy}$. Moreover, the GF components G^{00}_{zz} and G^{00}_{xx} which are needed for the calculation of $\Delta f^{(1)}_{zz}$ and $\Delta f^{(1)}_{xx}$ transform according to different irreducible representations of the D_{3h} group; hence these components could be calculated independently of equation (9). Such symmetry enables one to generalize the usual procedure of muffin-tin calculations to accommodate layered systems. The proposed generalization is necessary because the real potentials of layered systems are very anisotropic especially in the interstitial volume. Indeed, the potential averaged along the electron paths joining the atoms belonging to one layer is essentially more

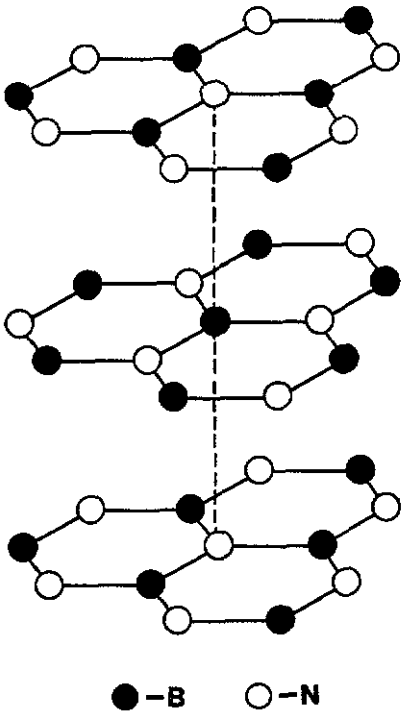

Figure 2. The 39-atom cluster of the h-BN crystal used in the calculations.

attractive than that averaged along the paths joining the atoms of different layers. Therefore the virtual electrons scattered from the atoms which belong to the same layer as the emitting atom, and electrons with the same energy scattered from atoms of neighbouring layers should have different average wave vector values in the interstitial region. If 1s electrons are excited into a continuum they move, for the most part, along the electric field vector of the incident radiation. Hence the average interstitial potential used for G_{xx}^{00} calculations must be chosen to be more attractive than that used for G_{zz}^{00} calculations.

The system of equations (9) has been solved for the 39-atom cluster shown in figure 2, and the scattering factor has been determined for the central boron atom of this cluster. Angular momenta of up to $l = 2$ for all atoms have been taken into account in calculations. The Herman–Skillman algorithm [21] with exchange parameters chosen according to Schwarz [22] was employed to calculate the atomic potentials. Atomic-sphere radii in the cluster were chosen to be equal to 0.75 Å for boron atoms and 0.7 Å for nitrogen atoms. Outside the cluster, the potential was chosen to be equal to the averaged interstitial potential (extended continuum model [23]). In order to investigate the influence of an inner 1s hole on the ASF, two calculations with different central-atom electron configurations were carried out: (i) all atoms in the cluster were considered to be neutral in the ground state, (ii) the configuration of the central boron atom was chosen to be $1s^1 2s^2 2p^2$ so as to take into account 1s hole and electron screening processes including extratomic screening.

The interstitial potential value used for the calculation of G_{xx}^{00} was obtained by averaging the potential over the interstitial volume of the sphere encompassing a boron

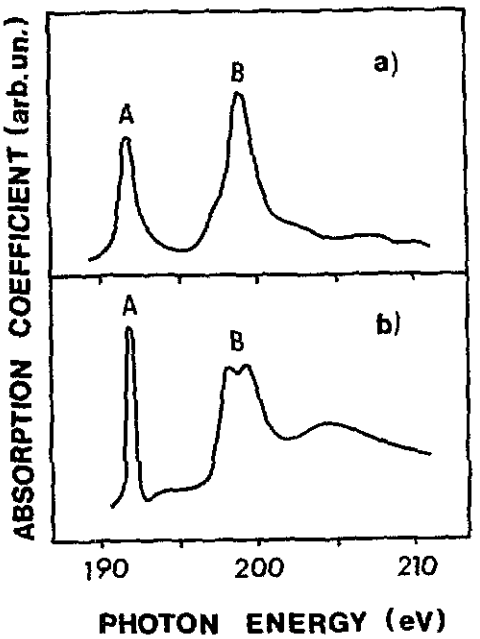

Figure 3. Theoretical (*a*) and experimental (*b*) [17] B K-edge XANES of the polycrystal h-BN sample.

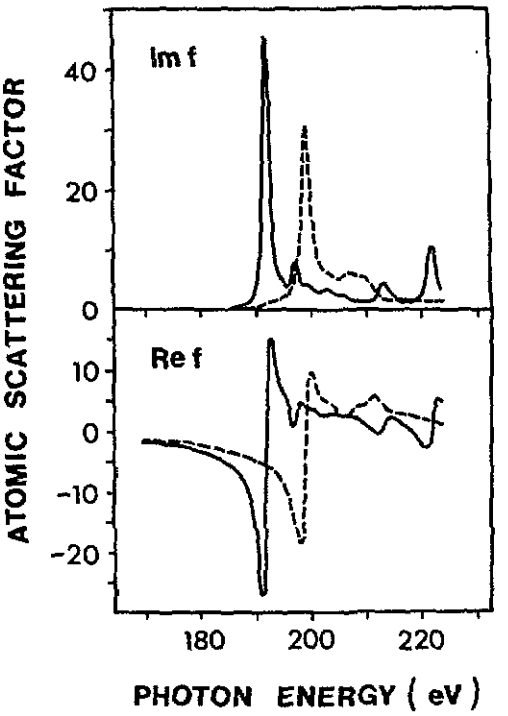

Figure 4. Imaginary and real parts of the anomalous correction to boron ASF tensor components f_{zz} (solid lines) and $f_{xx} = f_{yy}$ (dashed lines) in the h-BN crystal near the boron K edge.

atom and six nearest nitrogen atoms. The interstitial potential value used in the G_{zz}^{00} calculation was obtained by averaging the potential over the interatomic segment of the line joining the nearest atomic spheres in the different layers. The difference in the interstitial potentials calculated in such a way appeared to about 4 eV. The difference obtained confirms the opinion that the traditional muffin-tin approximation is not good enough for layered systems. In order to examine whether the generalization proposed above is appropriate in this case, the fine structure of the B K absorption spectrum in h-BN was calculated and compared with experiment [17]. The comparison of theoretical and experimental spectra obtained for a polycrystal sample is shown in figure 3. One can see that the main features of the theoretical spectrum (peaks A and B) agree well in their positions and relative intensities with those of the experimental spectrum if core-hole potential and electron screening are taken into account. This result confirms the calculation method proposed above.

Our calculations show that peak A is caused by the singularity in $G_{zz}^{nn}(\varepsilon)$ and peak B is caused by that in $G_{xx}^{nn}(\varepsilon)$. This conclusion is confirmed by B K-edge XANES angular dependence experimentally obtained for a h-BN monocrystal [18, 19]. It is interesting to note that peak A, caused by the electron transition to the bound state, appeared in the forbidden gap due to the influence of the 1s hole potential; so this peak represents the x-ray exiton and its width is determined entirely by many-electron effects.

The calculated anomalous corrections to the scattering factor tensor components of the boron atom in a h-BN crystal are shown in figure 4. The observed fine structure of

the scattering factor is caused by the scattering of the virtual electrons from the atoms surrounding the scattering one. Similar scattering of the photoelectrons causes x-ray absorption fine structure. The influence of the virtual electron scattering on the ASF is usually strong in the near edge region whereas in the EXAFS region, when photon energy exceeds the absorption edge by more than 20–50 eV, this scattering causes only weak oscillations of the ASF which are described by (15). Nevertheless, as it will be shown in the following section, the analysis of these oscillations could provide important information about the atomic structure of amorphous media.

The results obtained show that, in the near edge region, there are often sharp peaks in the ASF caused by virtual electron scattering from neighbouring atoms. The peak values of the VESC sometimes exceed the normal contributions to the ASF significantly and could be large enough to allow confident observation of the contribution to the x-ray scattering intensity from the atoms of low-Z elements. Of course it is necessary to recognize that the calculated peak values of the ASF are determined to a considerable extent by the value of the intermediate state width Γ especially for the exitonic peak A. We considered the value of Γ to be approximately equal to the width of the exitonic peak in the experimental B K x-ray absorption spectrum [17].

It is worth noting, too, that the anomalous correction f^{an} and the normal part f^{norm} of the isolated atomic-sphere scattering factor differ to some extent from those of a free neutral atom. The difference in the anomalous corrections is caused by the dissimilarity of the virtual electron wave functions calculated using the different potentials of the isolated atomic sphere and the free atom. The difference in the ASF normal parts is due to the lack of identity of the electron density distributions in the isolated atom and in the corresponding atom in the crystal.

4. Extended fine structure of the ASF and determination of the atomic ternary distribution function in amorphous media

In this section x-ray scattering from thin homoatomic amorphous samples is treated. The intensity of the scattered radiation is calculated above the K absorption edge in the EXAFS region. It is shown that this intensity is determined by pair and ternary atomic distribution functions that enable one to obtain information about the ternary distribution function in amorphous media from experimental spectra. Atomic ternary distribution functions (ATDFs) and, simply connected with them, atomic ternary correlation functions are of great interest for the theory of amorphous-media atomic structures [24]. A number of papers have been devoted to the problem of ATDF determination by EXAFS spectroscopy [25–27]. Unfortunately the x-ray absorption cross-section is a function of radiation frequency only, whereas the ATDF depends on three scalar arguments in homogeneous and isotropic media. Due to this fact, the method of ATDF analysis by means of EXAFS spectroscopy is restricted in principle. In the present paper a new approach to obtaining additional information about ATDF is proposed which is based on the analysis of the frequency dependence of the x-ray scattering intensity in the EXAFS region.

The angular distribution of x-ray diffraction in a normal dispersion region is determined entirely by the atomic pair distribution function (APDF). This well known result depends on the independence of the ASF on the position and chemical state of the scattering atoms in condensed matter when the photon energy is far from any absorption edge. As was shown in section 2, in the near edge region the ASF is the anisotropic tensor

which depends on the short-range atomic order due to virtual electron scattering from the scattering atom's neighbours (7). Therefore, in this region the intensity of the scattered radiation depends upon atomic correlation functions of orders higher than two. The simplest result takes place in the region of extended fine structure (50–1000 eV above the K edge) where the single-scattering approximation successfully takes into account the interaction of the virtual electrons with the neighbouring atoms. In this case, the simple expression (15) for the VESC can be used. Let us calculate the intensity of the radiation scattered from a thin homoatomic amorphous sample in the EXAFS region of photon energy. The component α of the electric field vector $\mathscr{E}$ of the radiation scattered from a single atom to the direction $\boldsymbol{n}$ can be written as follows [1]:

$$\mathscr{E}_\alpha = \frac{r_0}{R}\sum_{\beta,\gamma}(n_\alpha n_\beta - \delta_{\alpha\beta})f_{\beta\gamma}(r)\mathscr{E}_\gamma^{(0)}\,e^{-is\cdot r} \tag{16}$$

where $\mathscr{E}^{(0)}$ is the vector of the incident wave electric field, s is the diffraction vector, R is the distance between the sample and the detector, vector $\boldsymbol{r}$ defines the atom position in the sample and n_α is the component of the unit vector $\boldsymbol{n}$.

If the sample analysed is thin enough that x-ray absorption in it may be neglected, the intensity of the radiation scattered from the sample can be obtained easily from formula (16):

$$I(\omega,s) = \frac{c}{8\pi}\sum_\alpha|\mathscr{E}_\alpha|^2 = \frac{c}{8\pi}\left(\frac{r_0}{R}\right)^2\sum_{\alpha,\beta,\mu,\lambda}(\delta_{\alpha\beta}-n_\alpha n_\beta) \times\sum_{p,q}f^*_{\alpha\mu}(\omega,r_p)f_{\beta\lambda}(\omega,r_q)e^{is\cdot r_{qp}}\mathscr{E}_\mu^{(0)*}\mathscr{E}_\lambda^{(0)} \tag{17}$$

where summation over p and q extends over all atom numbers in the sample.

In the EXAFS region, the contribution from the VESC to the ASF is much smaller than the atomic one, f^{isol}; hence, substituting (12) and (15) for the last formula and neglecting the terms proportional to $F^2(\pi)$, one obtains

$$I = \frac{c}{8\pi}\left(\frac{r_0}{R}\right)^2\sum_{\alpha,\beta}(\delta_{\alpha\beta}-n_\alpha n_\beta)\left\{\sum_{p,q}e^{is\cdot r_{qp}}|f^{\text{isol}}|^2\mathscr{E}_\alpha^{(0)*}\mathscr{E}_\beta^{(0)} + \sum_\lambda f^{\text{isol}*}T_{\beta\lambda}\mathscr{E}_\alpha^{(0)*}\mathscr{E}_\lambda^{(0)} + \sum_\lambda f^{\text{isol}}T_{\alpha\lambda}\mathscr{E}_\lambda^{(0)*}\mathscr{E}_\beta^{(0)}\right\} \tag{18}$$

where

$$T_{\alpha\beta} = \sum_{p,q}\Delta f^{(1)}_{\alpha\beta}(r_q)\exp(is\cdot r_{qp}). \tag{19}$$

The first term in the braces has a well known form [24] whereas the last two terms describe the VESC influence on the scattered radiation intensity.

Let the coordinate system be chosen in such a way that the z-axis is directed along the wave vector of the incident beam and the x-axis is directed along its electric field vector. Let us determine x-ray scattering intensities for the scattering planes combined with xz and yz planes (p and s polarization of the incident beam). These intensities could be obtained from the expression (18) taking into account that in both cases $\mathscr{E}_y^{(0)} = \mathscr{E}_z^{(0)} = 0$, so the intensity I_0 of the incoming beam is equal to $(1/8\pi)(\mathscr{E}_x^{(0)})^2$. If 2θ is the scattering angle, then $n_x = \sin(2\theta)$, $n_y = 0$, $n_z = \cos(2\theta)$ for p polarization and

$n_x = 0, n_y = \sin(2\theta), n_z = \cos(2\theta)$ for s polarization. With the help of equation (18), one obtains:

$$I_p = I_0 \left(\frac{r_0}{R}\right)^2 \cos(2\theta) \left\{ |f^{isol}|^2 \sum_{p,q} e^{is\cdot r_{qp}} + 2\mathrm{Re}\left[(f^{isol})^*(T_{xx}\cos(2\theta) - T_{zx}\sin(2\theta))\right]\right\} \tag{20}$$

for p polarization, and

$$I_s = I_0 \left(\frac{r_0}{R}\right)^2 \left\{ |f^{isol}|^2 \sum_{p,q} e^{is\cdot r_{qp}} + 2\mathrm{Re}\left[(f^{isol})^* T_{xx}\right]\right\} \tag{21}$$

for s polarization.

For the isotropic sample it is convenient to calculate the tensor $T_{\alpha\beta}$ using another coordinate system (x', y', z') with the z'-axis directed along the diffraction vector s. In this case the tensor $T_{\alpha\beta}$ is obviously diagonal and $T_{x'x'} = T_{y'y'}$. Denoting $T_{z'z'} = T_1$ and $T_{x'x'} = T_{y'y'} = T_2$ one can obtain from (20) and (21) the following expressions:

$$I_p(\omega, s) = I_0 \left(\frac{r_0}{R}\right)^2 \cos(2\theta) \left\{ |f^{isol}|^2 \sum_{p,q} e^{is\cdot r_{qp}} + 2\mathrm{Re}[(f^{isol})^*(T_1\cos^2\theta - T_2\sin^2\theta)]\right\} \tag{22}$$

$$I_s(\omega, s) = I_0 \left(\frac{r_0}{R}\right)^2 \left\{ |f^{isol}|^2 \sum_{p,q} e^{is\cdot r_{qp}} + 2\mathrm{Re}\left[(f^{isol})^* T_2\right]\right\}. \tag{23}$$

In order to calculate the components T_1 and T_2 one needs to substitute (15) for (19):

$$T_1 = \sum_q \sum_p \sum_{n\neq q} \left\{ \left(\frac{2m\omega M_{01}}{\hbar}\right)^2 (r_{qn})_{z'}^2 \exp\left[2ikr_{qn} + 2i\delta_1 - \frac{m\Gamma r_{qn}}{k\hbar^2}\right] F(\pi)/r_{qn}^4 \right\} e^{is\cdot r_{qp}}$$

$$= \left(\frac{2m\omega M_{01}}{\hbar}\right)^2 F(\pi) e^{2i\delta_1} \sum_q \sum_p \sum_{n\neq q} u(r_{qn}, r_{qp}) \tag{24}$$

where

$$u(r_{qn}, r_{qp}) = (r_{qn})_{z'}^2 \exp[2ikr_{qn} - m\Gamma r_{qn}/k\hbar^2 + is\cdot r_{qp}]/r_{qn}^4.$$

Exploiting the relation $T_2 = \frac{1}{2}(T_{x'x'} + T_{y'y'})$ one can obtain the expression for T_2 from that for T_1 by introducing the expression $\frac{1}{2}[(r_{qn})_{x'}^2 + (r_{qn})_{y'}^2]$ in (24) instead of $(r_{qn})_{z'}^2$.

In the case of amorphous media, the expressions (22) and (23) for the scattered radiation intensities have to be averaged over all possible atomic configurations in the sample. As follows from these formulae, the intensities needed are the linear functions of the components of the tensor **T**. So in order to obtain the averaged intensities one should average the expressions for these components. Of course, the sum $\Sigma_{p,q} e^{is\cdot r_{qp}}$ appearing in (22) and (23) has to be averaged too. As is well known, such averaging is performed with the help of atomic distribution functions [24]. In homogeneous and isotropic media, the APDF $g(r)$ depends only on the distance between two atoms and the ATDF $g(r_1, r_2, \gamma)$ depends on three scalar arguments which determine the atomic triangle. We shall consider two sides—r_1 and r_2—and the angle between them, γ, to be the

arguments of the ATDF. The atomic distribution functions used in this paper are normalized by their asymptotic behaviour [24]

$$\begin{aligned} &g(r) \to 1 && \text{if } r \to \infty \\ &g(r_1, r_2, \gamma) \to g(r_1) && \text{if } r_2 \to \infty \text{ and } |r_1 - r_2| \to \infty. \end{aligned} \tag{25}$$

Before averaging it is convenient to divide the members of the sum over q, p and n in (24) into three groups: (i) $q = p, q \neq n$; (ii) $q \neq p, n = p$ and (iii) $q \neq p \neq n$.

$$\sum_q \sum_p \sum_{n \neq q} u(r_{qn}, r_{qp}) = \sum_q \sum_{n \neq q} u(r_{qn}, r_{qq}) + \sum_q \sum_{p \neq q} u(r_{qp}, r_{qp}) + \sum_q \sum_{p \neq q} \sum_{\substack{n \neq q \\ n \neq p}} u(r_{qn}, r_{qp}). \tag{26}$$

The sum over two non-equal atomic numbers after averaging transforms into the integral with APDF according to the usual rule. For instance:

$$\left\langle \sum_q \sum_{p \neq q} u(r_{qp}) \right\rangle = N\rho \int u(r) g(r)\, \mathrm{d}^3 r \tag{27}$$

where N is the total number of atoms in the sample and ρ is the atomic density.

The sum over three non-equal atomic numbers after averaging transforms into the integral with ATDF:

$$\left\langle \sum_q \sum_{p \neq q} \sum_{\substack{n \neq q \\ n \neq p}} u(r_{qn}, r_{qp}) \right\rangle = N\rho^2 \int u(r_1, r_2) g(r_1, r_2, \lambda)\, \mathrm{d}^3 r_1\, \mathrm{d}^3 r_2 \tag{28}$$

where λ is the angle between the vectors r_1 and r_2.

Using (26)–(28) one can easily obtain the averaged value of T_1:

$$\begin{aligned} \langle T_1 \rangle = \left(\frac{2m\omega M_{01}}{\hbar}\right)^2 F(\pi)\, \mathrm{e}^{2\mathrm{i}\delta_1} N\rho \Bigg\{ & 2\pi \int \cos^2\theta_1 \exp\left(2\mathrm{i}kr_1 - \frac{m\Gamma}{k\hbar^2} r_1\right) \\ & \times \left[1 + \exp(\mathrm{i}sr_1 \cos\theta_1)\right] g(r_1)\, \mathrm{d}r_1\, \mathrm{d}\cos\theta_1 \\ & + \rho \int\int \cos^2\theta_1 \exp\left(2\mathrm{i}kr_1 - \frac{m\Gamma}{k\hbar^2} r_1\right) \exp(\mathrm{i}sr_2 \cos\theta_2) \\ & \times g(r_1, r_2, \lambda) r_2^2\, \mathrm{d}r_1\, \mathrm{d}\cos\theta_1\, \mathrm{d}\varphi_1\, \mathrm{d}r_2\, \mathrm{d}\cos\theta_2\, \mathrm{d}\varphi \Bigg\} \end{aligned} \tag{29}$$

where $\cos\lambda = \cos\theta_1 \cos\theta_2 + \sin\theta_1 \sin\theta_2 \cos(\varphi_2 - \varphi_1)$ and $\varphi = \varphi_2 - \varphi_1$.

The averaged component T_2 can be obtained from (29) by replacing the term $\cos^2\theta_1$ in the beginning of the integrands in (29) by $\frac{1}{2}\sin^2\theta_1$.

When one performs averaging of the sum $\Sigma_{p,q}\, \mathrm{e}^{\mathrm{i}s \cdot r_{qp}}$, the expression similar to (27) can also be exploited, but an atomic correlation function $h(r) = g(r) - 1$ is usually substituted for the integrand instead of an atomic distribution function. Such replacement is caused by the divergence of the integral (27) in the case of infinite sample volume and does not change the result beyond the region of small scattering angles [24]. The result of such averaging is usually called the structure factor.

When one averages the tensor components T_i the integrals containing the APDF are convergent due to the non-zero width, Γ, of the intermediate state that causes

exponential decreasing of the integrands as follows from (24). The integrand containing the ATDF decreases rapidly when $r_1 \to \infty$ but the integration over r_2 leads to a value proportional to the sample volume in the region of small scattering angles. Just as in the case of the structure factor calculation, it is possible to change the integrand in (29) and obtain a rapidly decreasing function without changing the result, with the exception of the small-angle region.

In order to do this, one should use the difference $g(r_1, r_2, \gamma) - g(r_1)$ instead of the ATDF. According to (25) such a difference decreases when r_2 increases, and the integral treated appears to be convergent. Now one can write the expressions for scattered radiation intensities in the final form

$$I_p(\omega, s) = I_0(r_0/R)^2 \cos(2\theta) N\Big\{|f^{isol}|^2 \Big[1 + (4\pi\rho/s)\int h(r)\sin(sr)\, r\, dr\Big]$$
$$+ \mathrm{Re}\Big\{\Big(\frac{4m\omega M_{01}}{\hbar}\Big)^2 \pi\rho F(\pi)\, e^{2i\delta_1}(f^{isol})^* \Big[\int g(r)\exp\Big(2ikr - \frac{m\Gamma}{k\hbar^2}r\Big)$$
$$\times (f_1(sr)\cos^2\theta - f_2(sr)\sin^2\theta)\, dr$$
$$+ \rho\int\int\Big(g(r_1, r_2, \gamma) - g(r_1)\Big)\exp\Big(2ikr_1 - \frac{m\Gamma}{k\hbar^2}r_1\Big)\exp(isr_2\cos\theta_2)$$
$$\times (\cos^2\theta_1\cos^2\theta - \tfrac{1}{2}\sin^2\theta_1\sin^2\theta)\, r_2^2\, dr_1\, d\cos\theta_1\, dr_2\, d\cos\theta_2\, d\varphi\Big]\Big\}\Big\} \tag{30}$$

$$I_s(\omega, s) = I_0(r_0/R)^2 N\Big\{|f^{isol}|^2\Big[1 + (4\pi\rho/s)\int h(r)\sin(sr)\, r\, dr\Big]$$
$$+ \mathrm{Re}\Big(\frac{4m\omega M_{01}}{\hbar}\Big)^2 \pi\rho F(\pi)\, e^{2i\delta_1}(f^{isol})^*$$
$$\times \Big[\int g(r)\exp\Big(2ikr - \frac{m\Gamma}{k\hbar^2}r\Big) f_2(sr)\, dr$$
$$+ \rho\int\int\Big(g(r_1, r_2, \gamma) - g(r_1)\Big)\exp\Big(2ikr_1 - \frac{m\Gamma}{k\hbar^2}r_1\Big)\exp(isr_2\cos\theta_2)$$
$$\times \tfrac{1}{2}\sin^2\theta_1\, r_2^2\, dr_1\, d\cos\theta_1\, dr_2\, d\cos\theta_2\, d\varphi\Big]\Big\} \tag{31}$$

where

$$f_1(x) = \int_0^\pi \cos^2\theta(1 + e^{ix\cos\theta})\sin\theta\, d\theta = \tfrac{2}{3} + \sin x/x + 2\cos x/x^2 - 2\sin x/x^3$$

$$f_2(x) = \int_0^\pi \tfrac{1}{2}\sin^2\theta(1 + e^{ix\cos\theta})\sin\theta\, d\theta = \tfrac{2}{3} + \sin x/2x - \cos x/x^2 + \sin x/x^3.$$

To transform the formulae (22) and (23) into (30) and (31) we have used the traditional expression for the structure factor [24]:

$$1 + (4\pi\rho/s)\int h(r)\sin(sr) r\, dr$$

and have carried out the integration over θ_1. One can see from (30) and (31) that the

intensity of x-ray diffraction in the anomalous dispersion region is the sum of the terms with different origin which have quite unsimilar dependences on radiation frequency. The first terms in (30) and (31) are the traditional ones, which are determined by the scattering factors of isolated atomic spheres f^{isol} and APDF. The other terms appear to be due to VESC. They depend on both APDF and ATDF. The magnitudes of these terms are about a few percent of the first-term magnitudes of the low-energy side of the EXAFS region and fall with increasing radiation frequency. Nevertheless, the terms caused by VESC could be determined confidently from the experimental signal because of the quite different character of their frequency dependence compared to that of the traditional terms. Indeed, let one measure the frequency dependence of the diffraction intensities so as to keep the diffraction vector constant. In the EXAFS region, the scattering factor f^{isol} may be considered to depend on the diffraction vector only, therefore the intensity of normal diffraction measured in such a way does not depend on radiation frequency at all. In contrast, the terms caused by the VESC show fast oscillations due to the factor $\exp(2ikr)$. The methods of decomposition of smooth and oscillatory signals are developed in EXAFS theory. After determination of the terms caused by VESC one could exclude the contributions due to the APDF and obtain in such a way the terms which depend on the ATDF. Unfortunately, these terms are functions of two variables only: ω and s whereas the ATDF is a function of three variables. So it is impossible to determine the ATDF directly from experimental data; however, different models for the ATDF could be tested. As one can see from expressions (30) and (31) the experiments with s and p polarized incident beams give complementary information about the ATDF so both should be used to obtain the ATDF. The scattering intensity measurement of an incident wave having an arbitrary polarization vector direction gives no additional information. Indeed, such a wave can be treated as the superposition of two waves with electric field vectors perpendicular and parallel to the scattering plane. As follows from (16), this property is conserved for the electric field vectors of corresponding scattered waves as well. Therefore, the averaged intensity of the radiation scattered from an amorphous sample in any direction is the linear combination of the intensities $I_p(\omega, s)$ (equation (30)) and $I_s(\omega, s)$ (equation (31)).

If one employs the intensities $I_p(\omega, s)$ and $I_s(\omega, s)$ to get information about the ATDF it is necessary to first estimate the intervals where the arguments ω and s vary. The wider these intervals the more precise the information obtained about the ATDF. The interval of the photon energy, $\hbar\omega$, is almost the same as in the EXAFS investigation, i.e. from about 50 eV above the 1s threshold up to the value at which the signal to noise relation is not too small. This value is usually about several hundred electron volts. The interval of the diffraction vector modulus s variation depends on the atomic number Z of the atom investigated because the photon energy is close to the K absorption edge of this atom. Hence the maximum value of s is about $E_{1s}/\hbar c$ and it increases with the growth of Z. On the other hand, the 1s level width also increases with the growth of Z that causes ASF fine-structure suppression. Taking into account these restrictions, amorphous germanium seems to be very suitable for investigation of the ATDF by the method proposed in this paper.

References

[1] James R W 1950 *The Optical Principles of the Diffraction of X-rays* vol 2, ed L Bragg (London)
[2] Belyakov V A 1975 *Usp. Fiz. Nauk* **115** 533; 1975 *Sov. Phys. Usp.* **18** 267

[3] Dmitrienko V E 1984 *Acta Crystallogr.* A **40** 89
[4] Brouder C 1990 *J. Phys.: Condens. Matter* **2** 701
[5] Filatova E O, Blagovechenskaya T A and Kozhahmetov S K 1990 *Fiz. Tverd. Tela* **32** 1551
[6] Martens G and Rabe P 1980 *Phys. Status Solidi* a **58** 415
[7] Martens G and Rabe P 1981 *J. Phys. C: Solid State Phys.* **14** 1524
[8] Ponomarev Yu V and Turutin Yu A 1984 *J. Tekh. Phis.* **54** 391
[9] Ashley C A and Doniach S 1975 *Phys. Rev.* B **11** 1279
[10] Vedrinskii R V and Novakovich A A 1975 *Fiz. Metallov. Metalloved.* **39** 7
[11] Taylor J R 1972 *Scattering Theory* (NY, London, Sydney, Toronto: Wiley)
[12] Koningsberger D C and Prins R (ed) *X-ray Absorption, Principles, Applications, Techniques of EXAFS, SEXAFS and XANES* (New York: Wiley)
[13] Lee P A and Pendry J B 1975 *Phys. Rev.* B **11** 2795
[14] Teo B K 1981 *J. Am. Chem. Soc.* **103** 3990
[15] Vedrinskii R V and Kraizman V L 1976 *Izv. Akad. Nauk. SSSR* **40** 248
[16] Kochubey D I *et al* 1988 *Rentgeno-spectralny Method Izucheniya Structuri Amorfnih Tel* (Novosibirsk: Nauka)
[17] Fomichev V A 1967 *Fiz. Tverd. Tela* **9** 3167 (Engl. Transl. 1968 *Sov. Phys.–Solid State* **9** 2496)
[18] Barth J, Kunz C and Zimkina T M 1980 *Solid State Commun.* **36** 453
[19] Davies B M, Bassani F and Brown F C 1981 *Phys. Rev.* B **24** 3537
[20] Hoffman D M, Doll G L and Eclund P C 1984 *Phys. Rev.* B **30** 6051
[21] Herman F and Skillman S 1963 *Atomic Structure Calculation* (Englewood Cliffs, NJ: Prentice-Hall)
[22] Schwarz K 1972 *Phys. Rev* B **5** 2466
[23] Doniach S, Berding M, Smith T and Hodgson K O 1984 *EXAFS and Near Edge Structure III* ed K O Hodgson, B Hedman and J E Penner-Hahn (Berlin: Springer) p 33
[24] Ziman J M 1979 *Models of Disorder* (Cambridge: Cambridge University Press)
[25] Benfatto M, Natoli CR, Bianconi A, Garcia J, Marcelly A, Fanfoni M and Davoli I 1986 *Phys. Rev.* B **34** 5774
[26] Bianconi A, Garcia J and Benfatto M 1988 *XANES in Condensed Systems (Topics in Current Chemistry 145)* (Berlin: Springer) p 30
[27] Filipponi A, Cicco A Di, Benfatto M and Natoli C R 1990 *Europhys. Lett.* **13** 319